Chapter 10
Twisted Light in Supercontinuum: From Self-Phase Modulation to Superfluidity in Kerr Medium

J. T. Mendonça

Abstract This chapter considers the influence of laser pulse topology on the formation of a supercontinuum. This occurs when the usual Gaussian laser pulses are replaced by twisted pulses, which carry a finite amount of orbital angular momentum (OAM). Generation of ring-shaped and of helical pulses with a broad spectrum is discussed. We also study the possible relation between self-phase modulation (SPM), which is at the origin of the supercontinuum, and the superfluidity of light. These two phenomena can occur in a Kerr medium. For short pulses and long propagation distances, SPM could modify the conditions for the observation of superfluid light.

Keywords Photon OAM · Self-phase modulation · Superfluidity · Kerr medium

10.1 Introduction

Self-phase modulation (SPM) of a short laser pulse, which is at the origin of the so-called supercontinuum, is presently well understood (Boyd, 1992; Alfano, 2016; Alfano & Shapiro, 1970). The supercontinuum arises from the nonlinear change in the refractive index which occurs in a Kerr medium. In a recent work Mendonça (2020), we have extended SPM to the case of twisted laser pulses from OAM, a topic which became popular in the modern literature (Secor et al., 2017; Yao & Padgett, 2011). It is well-known that twisted laser pulses carry a finite amount of orbital angular momentum and possess remarkable nonlinear properties (Mendonça et al., 2009; Zhu et al., 2018).

In this chapter, we review SPM and the supercontinuum of twisted laser pulses and discuss two different pulse configurations. One is that of a single twisted mode, characterized by a single topological charge l, and corresponds to a donut or

J. T. Mendonça (✉)
Instituto Superior Técnico, Universidade de Lisboa, Lisbon, Portugal
e-mail: titomend@tecnico.ulisboa.pt

R. R. Alfano (ed.), *The Supercontinuum Laser Source*,
https://doi.org/10.1007/978-3-031-06197-4_10

ring-shaped helical intensity distribution. The other is that of mode superposition, particularly that of light springs (Pariente and Quéré, 2015), which corresponds to a helical energy distribution, and contains two or more topological charges. Light springs are particularly important because they are able to accelerate helical electron beams (Vieira et al., 2018).

We also relate SPM with the superfluidity of light, another possible process in a nonlinear Kerr medium. The interest on superfluid light emerged in recent years, as an alternative experimental approach to condensed matter processes (Carusoto & Ciuti, 2013; Bolda et al., 2001; Chiao & Boyce, 1999). This effect is associated with the disappearance of diffraction produced by optical obstacles and can occur for sufficiently intense laser beams. Nonlinear inhibition of diffraction is the main signature of superfluidity, when light becomes insensitive to small optical obstacles. Several experimental arrangements have been proposed (Lerario et al., 2017; Michel et al., 2018; Silva et al., 2017; Rodrigues et al., 2020). The standard theoretical models of superfluid light usually ignore the influence of pulse duration. But, for short pulses, nonlinear frequency shifts associated with SPM could eventually interfere with superfluidity. In that case, SPM could modify the basic properties of the photon fluid and, as a result, introduce qualitative changes in the fluid-superfluid transition, due to its sensitivity to frequency and intensity space-time distributions.

10.2 Ring-Shaped Supercontinuum

We first consider SPM in a twisted beam of light with topological charge l. This charge represents the orbital angular momentum of light in the forward direction. The corresponding transverse field profile is given by a radial Laguerre-Gauss (LG) function, for unbounded beam propagation, or by a radial Bessel function for fiber mode propagation. Let us then describe the field mode as:

$$\mathbf{E}\left(\mathbf{r},t\right)=\mathbf{e}_{\mathrm{l}}E_{\mathrm{l}}\left(\mathbf{r}_{\perp},z,t\right)\ \exp\ \left(i\phi_{\mathrm{l}}\left(\mathbf{r},t\right)\right), \tag{10.1}$$

where $\mathbf{e}_{\mathrm{l}}$ is the unit polarization vector, $E_{\mathrm{l}}(\mathbf{r}_{\perp},z,t)$ is a slowly varying amplitude, and $\phi_{\mathrm{l}}(\mathbf{r}_{\perp},z,t)$ is the total phase. We can write them explicitly as:

$$E_{\mathrm{l}}\left(\mathbf{r}_{\perp},z,t\right)=u\left(z,t\right)\mid F_{\mathrm{lp}}\left(\mathbf{r}_{\perp}\right)\mid, \tag{10.2}$$

where $u(z,t)$ is the mode amplitude profile and (l,p) are pairs of quantum numbers specifying the different LG modes. The mode number p gives the number of zeros in the radial direction, and will be considered equal to zero in the numerical examples given here, for simplicity. Using polar coordinates $\mathbf{r}_{\perp}=(r,\theta)$, we can write the LG functions as:

$$F_{\mathrm{lp}}\left(\mathbf{r}\perp\right)=C_{\mathrm{lp}}\ X^{|l|/2}L^{|l|}\mathrm{p}(X)\ \exp\ \left(-X/2+il\theta\right), \tag{10.3}$$

where L_p^1 are the associated Laguerre polynomials with argument $X = r^2/w^2$ and w defines the laser beam waist. Note that this quantity is slowly varying along propagation but can be assumed nearly constant inside of the focal region, over a distance of the order of the Rayleigh length. This is valid for unbounded media. The normalization factors C_{lp} are used to satisfy the orthonormal relations between modes, as defined by:

$$\int_0^\infty r\, dr \int_0^{2\pi} d\Theta\, F_{lp}^*(r,\Theta)\, F_{l'p'}(r,\Theta) = \delta_{ll'}\delta_{pp'}. \tag{10.4}$$

A similar description can be used for optical fibers, but using radial Bessel functions, instead of the above LG functions. The field phase in Eq. (10.1) is given by:

$$\phi_l(\mathbf{r},t) = l\theta + (kz - \omega t), \tag{10.5}$$

where the frequency ω is related to the wavenumber by the nonlinear dispersion relation:

$$\omega = \frac{kc}{\sqrt{\epsilon(\omega)}}\left[1 - \alpha(\omega)|E|^2\right], \tag{10.6}$$

with:

$$\epsilon(\omega) = 1 + \chi^{(1)}(\omega), \qquad \alpha(\omega) = \frac{\omega\, v_k}{2kc^2}\chi^{(3)}, \tag{10.7}$$

where $\chi^{(1)}$ and $\chi^{(3)}$ are the linear and the Kerr susceptibilities, respectively. The resulting nonlinear dependence of the phase on the field intensity leads to a radially symmetric frequency shift, determined by the expression:

$$\omega(t) = \omega_0\left\{1 + \alpha\frac{t}{v_0}\left|F_{lp}(\boldsymbol{r}_\perp)\right|^2\frac{\partial}{\partial\eta}|u(\eta)|^2\right\}. \tag{10.8}$$

Here, $\omega_0 = \omega(t=0)$ is the initial pulse frequency, $\eta = (z - v_0 t)$ is the space variable in the pulse reference frame, and v_0 is the linear group velocity. SFM and the subsequent generation of the supercontinuum will therefore depend on the radial pulse profile, as determined by the new factor $|F_{lp}(\mathbf{r}_\perp)|^2$. Noting that the intensity profile is independent of the angular variable θ, this will lead to a donut or ring-shaped frequency shift, as illustrated in Fig. 10.1. Here, we have used a Gaussian envelope profile, as determined by $|u(\eta)| = u_0 \exp.(-\eta^2/2\sigma^2)$, where σ determines the pulse duration.

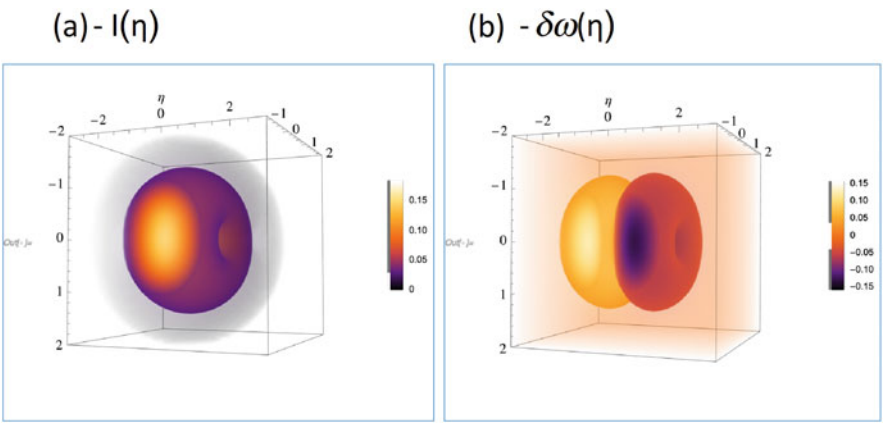

Fig. 10.1 Three-dimensional representation of a twisted laser beam, described by the LG mode (l = 1, p = 0): (**a**) laser pulse intensity I(η); (**b**) frequency shift $\delta\omega(\eta)$, due to SPM inside the pulse. This configuration can lead to the formation of a ring-shaped white light

10.3 Helical Supercontinuum

Let us now consider the superposition of two different twisted modes, characterized by two distinct topological charges, or angular momentum quantum numbers, l_1 and l_2. In this case, Eq. (10.1) is replaced by:

$$\boldsymbol{E}\left(\boldsymbol{r},t\right)=\sum_{j=1,2}\boldsymbol{e}_{j}E_{j}\left(\boldsymbol{r}_{\perp},\eta\right)\ \exp\left[i\phi_{j}\left(\boldsymbol{r},t\right)\right], \tag{10.9}$$

With:

$$E_{j}\left(\boldsymbol{r}_{\perp},\eta\right)=u_{j}\left(\eta\right)\left|F_{j}\left(\boldsymbol{r}_{\perp}\right)\right|,\phi_{j}\left(\boldsymbol{r},t\right)=l_{j}\theta+\left(k_{j}z-\omega_{j}t\right), \tag{10.10}$$

We assume $\mathbf{e}_{\mathrm{j}}=\mathbf{e}$ and ignore polarization effects. Let us introduce the relative amplitude $R=E_2/E_1$. In general, this quantity depends on both the axial and radial variables, $R\equiv R(\mathbf{r}_{\perp},\ \eta)$, but in some useful cases, its radial dependence is small and can be ignored. The resulting pulse intensity will then be proportional to the quantity:

$$\left|E\left(\mathbf{r}_{\perp},\eta\right)\right|^{2}=\left|E_{1}\right|^{2}\left\{\left(1+R^{2}\right)+2R\ \cos\left(\delta_{1}\theta-\delta k\ z-\delta\omega\ t\right)\right\}, \tag{10.11}$$

with $\delta_1=l_1-l_2$, $\delta k=k_1-k_2$, and $\delta\omega=\omega_1-\omega_2$. For $\delta\omega\neq0$, we get the so-called light springs. These configurations are particularly useful for laser acceleration schemes, because they lead to the formation of energetic helical electron beams

(Vieira et al., 2018). The simplest example of a light spring corresponds to $R \simeq 1$, and $\delta_1 = 1$. The above expression is reduced to:

$$|E(\mathbf{r}_\perp, \eta)|^2 \simeq 2|E_1|^2 \left\{ \left(1 + \cos(\theta - \delta k\, z - \delta\omega\, t) \right\}, \tag{10.12}$$

The other interesting example is that of two modes with the same frequency, such that $\delta k = \delta\omega = 0$, but dephased in time. We get the self-torque configurations, recently discussed in Rego et al. (2019). They can be described by:

$$|E(\mathbf{r}_\perp, \eta)|^2 \simeq |E_1|^2 \left[1 + R(\eta)^2 \right] + 2R(\eta)\ \cos(\delta_1 \theta), \tag{10.13}$$

The interest of this new example of two temporally dephased modes is that the angular momentum seems to vary continuously inside the pulse, from l_1 to $l_2 \neq l_1$, due to the variation of their relative amplitudes.

The frequency shift originating from the light spring configuration of Eq. (10.12) is given by:

$$\omega(t) = \omega_0 \{1 + \overline{\alpha}\, t \cos(\theta - \delta k\, z - \delta\omega\, t)\}, \tag{10.14}$$

with the nonlinear factor:

$$\overline{\alpha} = \sum_{j=1,2} \frac{\alpha_j}{v_j} \left| F_j(r_\perp) \right|^2 \frac{\partial}{\partial \eta} |u(\eta)|^2. \tag{10.15}$$

Here, the pulse envelope was assumed identical for the two modes, $u_j(\eta) = u(\eta)$. This leads to the formation of a supercontinuum with new topological properties. The frequency space-time distribution follows a helical shape, similar to that of the pulse intensity, and is fundamentally different from that of a single twisted mode, because it now depends on both the transverse and the angular coordinates. These new features are illustrated in Fig. 10.2. Of particular interest is the topological similarity between the acceleration of helical electron beams, demonstrated in Vieira et al. (2018), and the formation of the helical frequency shifts shown in this figure. Similarities between particle acceleration and photon frequency shifts were noted long ago in plasma physics and led to the concept of photon acceleration [see Mendonça, 2001 and references therein].

Finally, for the self-torque configurations of Eq. (10.13), the SPM frequency shifts are determined by an expression of the form:

$$\omega(t) = \omega_0 \{1 + \nu_0 t + [2\mathrm{R} + \cos(\delta_1 \theta)]\ \nu_1 t\}, \tag{10.16}$$

where $\nu_0 \simeq \bar{\alpha}$ and $\nu_1 \propto (\partial R/\partial \eta)$. Here, the frequency distribution not only loses the axial symmetry of the single twisted mode case, shown in Fig. 10.1b, but also

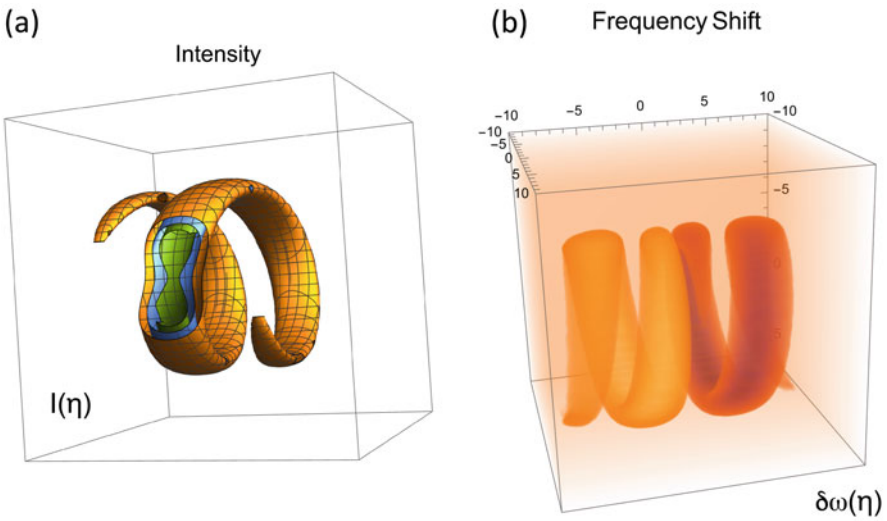

Fig. 10.2 Three-dimensional representation of a light spring, described by the superposition of two LG modes ($l = 6$, $p = 0$) and ($l = 7$, $p = 0$) with equal amplitude: (**a**) laser pulse intensity $I(\eta)$; (**b**) frequency shift $\delta\omega\,(\eta)$, due to SPM inside the spring

the helical property observed with light springs, shown in Fig. 10.2b. This lack of symmetry is due to the conditions ($\delta l \neq 0$, $\delta\omega = 0$), similar to those considered in Mendonça and Vieira (2014), and also to an additional contribution associated with v_1.

10.4 Superfluidity

We now briefly discuss the superfluidity of twisted laser pulses. It is well-known that pulse propagation in a Kerr medium satisfies a nonlinear equation of the form:

$$i\frac{\partial E}{\partial z} = -\left[\frac{1}{2k}\nabla_\perp^2 + \frac{k}{2\epsilon\,(\omega)}\chi^{(3)}|E|^2\right]E. \tag{10.17}$$

We should keep in mind that, for any given location inside the pulse, specified by η, the frequency will increase or decrease along propagation. But we are now more interested in the processes taking place in the perpendicular direction. Equation (10.17) is able to describe the evolution of perturbations in the perpendicular plane $\mathbf{r}_\perp$, during pulse propagation along the z direction. Noting that the center of the pulse moves with $\eta = 0$, or $z = v_0 t$, we can replace the axial variation along z by a temporal variation of the envelope. On the other hand, we can introduce a new

field function, $\psi(\mathbf{r}_\perp, t) = E(\mathbf{r}_\perp, z = \mathrm{v}_0 t)$, and reduce Eq. (10.17) to the standard nonlinear Schrödinger form:

$$i\hbar \frac{\partial}{\partial z}\psi = -\left[\frac{\hbar^2}{2m}\nabla_\perp^2 - g|\psi|^2\right]\psi. \tag{10.18}$$

The effective photon mass m, and coupling parameter g, appearing in this equation, are defined by:

$$m = \frac{\hbar k}{v_0}, \qquad g = -\frac{\hbar v_0}{c}\,\frac{\omega}{\sqrt{\epsilon\,(\omega)}}. \tag{10.19}$$

The Planck constant $\hbar$ was introduced for dimensional purposes. This is formally identical to the Gross-Pitaevskii equation used to describe Bose-Einstein condensates (Pethick and Smith, 2008), and we have chosen the sign of g according to the usual convention. The case of positive nonlinear susceptibility, $\chi^{(3)} > 0$, will correspond to condensates with attractive interactions, and the opposite case of a negative nonlinearity, $\chi^{(3)} < 0$, to repulsive condensates. At this point, it is useful to introduce a Madelung transformation, such that $\psi = \sqrt{n}\,\exp.\,(i\phi)$. This allows us to describe the laser pulse as a fluid, where the photon fluid density n and mean velocity $\mathbf{v}$ are defined as $n = |\psi|^2 = |E|^2$, and $\mathbf{v} = \nabla_\perp \phi$. From Eq. (10.18), we can then derive the corresponding fluid equations, similar to those of a condensate, as (Carusoto & Ciuti, 2013; Rodrigues et al., 2020):

$$\frac{\partial n}{\partial t} + \nabla_\perp\,(n\,\mathbf{v}) = 0, \quad \frac{\partial \mathbf{v}}{\partial t} + \mathbf{v}.\nabla_\perp\,\mathbf{v} = -\frac{g}{m}\,\nabla_\perp n + \frac{\hbar^2}{2m^2}\,\nabla_\perp\left(\frac{\nabla_\perp^2\sqrt{n}}{\sqrt{n}}\right), \tag{10.20}$$

Here, the laser pulse (or photon fluid) parameters m and g depend on the position η inside the laser pulse envelope. It should be noticed that the equilibrium values for the photon density and transverse velocity, n_0 and $\mathbf{v}_0$, are determined by the appropriate twisted mode structure. They will also depend on the frequency shifts associated with SPM, which result from the pulse propagation through the nonlinear medium. In that way, the fluid properties become dependent on the SPM process. For a single twisted mode, characterized by the topological charge l, these equilibrium values are:

$$n_0 = |u_l|^2\left|F_{lp}\,(r_\perp)\right|^2, \quad \mathrm{v}_0 = \nabla_\perp \phi = \frac{l}{r}\,e_\theta. \tag{10.21}$$

This equilibrium state corresponds to a concentric photon fluid ring, as represented in Fig. 10.1a, rotating with a finite polar velocity $\mathbf{v}_0 = \mathbf{v}_\theta$. The resulting transverse flow is proportional to the orbital angular momentum of the twisted beam, $\hbar\, l$, and vanishes for a purely Gaussian pulse.

Let us now assume some elementary perturbations inside these rotating rings of light, as defined by the perturbed quantities $\delta n = n - n_0$, and $\delta \mathbf{v} = \mathbf{v} - \mathbf{v}_0$. Assuming that these perturbed quantities are proportional to exp. $(i\mathbf{q}\cdot\mathbf{r}_\perp - i\Omega t)$, where $\mathbf{q}$ is the wave vector and Ω is the frequency, assumed very small with respect to the photon frequencies, $\Omega \ll \omega$, we can obtain after linearization of Eq. (10.20), a dispersion relation of the form:

$$(\Omega - \mathbf{v}_0.\mathbf{q})^2 = c_s^2 q^2 + \frac{\hbar^2 q^4}{4m^2}. \tag{10.22}$$

where $c_s = (g\ n_0/m)^{1/2}$ can be called the Bogoliubov speed of the photon fluid. Notice that this quantity depends parametrically on η, through the values of g and m, given by Eq. (10.19). It also depends on t, because the photon frequency $\omega(\eta)$ and wavenumber $k(\eta)$ evolve along propagation, and on the radial position as well, through the equilibrium density n_0. This shows that, even if this dispersion relation is formally identical to that of a moving Bose-Einstein condensate, its physical meaning is significantly different and that a more complex view of light superfluidity emerges when SPM is taken into account.

These elementary oscillations in the photon fluid reveal a possible transition to superfluidity, as shown next. Given the radial shape of this fluid, it is appropriate to consider purely poloidal oscillations, eventually relevant to experiments. In this case, we assume $\mathbf{q} = q_\theta \mathbf{e}_\theta$ and, due to the existence of periodic boundaries, we should also keep in mind that such oscillations typically evolve as $q_\theta \sim l'/w$, with $l' \gg l$. The dispersion relation (10.22) then becomes:

$$\left(\Omega - \frac{l q_\theta}{r}\right)^2 = \frac{g n_0\,(r_\perp)}{m}\, q_\theta^2 + \frac{\hbar^2 q_\theta^4}{4m^2}. \tag{10.23}$$

At this point, it is useful to invoke the Landau criterion (Pethick and Smith, 2008). It states that superfluidity will only occur if none of these acoustic type of oscillations can be excited. The photon flow in the poloidal direction will then become insensitive to any given obstacle. This is only possible when $v_\theta < c_s$, or in other terms, when the laser intensity $I \equiv n_0$ is larger than some critical value $I \geq I_c$, defined as:

$$I_c = \frac{l^2}{w^2}\,\frac{m}{g}. \tag{10.24}$$

It is clear that this quantity will depend on η and t, as well as on the radial position. This means that, sufficiently close to the optical axis, superfluidity will necessarily collapse, at a critical radius $r_c \leq l\ m/g$, thus creating a kind of moving horizon between the normal fluid and superfluid.

Let us now discuss the implications of our analysis to possible observation of superfluidity with SPM. For very long pulses, with duration $\Delta t = \sigma/v_0$, SPM can be ignored if the maximum frequency shift is smaller than the natural pulse width,

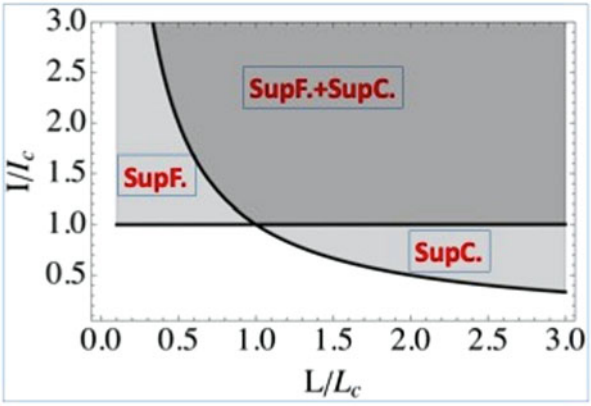

Fig. 10.3 Map of laser intensity versus propagation distance. Intensity is normalized to the critical intensity I_c for superfluidity; and distance is normalized to the critical distance L_c for supercontinuum. Three regions are identified for the observation of superfluidity alone, supercontinuum alone, and both

$\delta\omega_0 \simeq 1/\Delta t$. In this case, we can study superfluidity as an isolated phenomenon. This is no longer true for large propagation distances L, because the frequency shifts modify the value of this critical intensity, I_c. It is therefore useful to state a condition for the inclusion of SPM in the analysis of superfluid light. This can be approximately written as:

$$\Delta\omega \geq \alpha \frac{2\omega_0 \eta}{\sigma} n_0, \tag{10.25}$$

Assuming that maximum frequency shifts occur at a position $\eta \simeq \sigma$, we can establish a criterion for the occurrence of SPM in a superfluid experiment in terms of the propagation distance as $L \geq L_c$, where the critical distance is determined by:

$$L_c = \frac{v_0}{\alpha\omega_0 n_0}. \tag{10.26}$$

This means that, for sufficiently large laser pulse intensities $I \equiv n_0$, or alternatively, for sufficiently long distances L, the two effects of SPM and light superfluidity will eventually merge and will have to be considered simultaneously. However, for sufficiently long pulses, or sufficiently weak laser intensities, they can be observed separately, as it occurs in most experiments so far. The three possible experimental regions are illustrated in the (I, L) diagram of Fig. 10.3.

10.5 Conclusions

In this chapter, we have explored the new topological features of SPM and supercontinuum when twisted laser configurations are introduced, as well as their relations with the superfluid properties of light.

Twisted laser pulses carry a finite amount of orbital angular momentum, and the influence of their topological properties on the formation of a supercontinuum was discussed. Two main examples of twisted pulses were considered. One is that of simple twisted pulses, characterized by a single topological charge l. The other example corresponds to more complex pulses, such as those of light springs and self-torque configurations proposed in recent years. They result from the superposition of two (or more) twisted modes with different topological charges and frequencies. Simple twisted pulses lead to ring-shaped frequency profiles, whereas more complex pulses can lead to helical-shaped or to asymmetric frequency profiles. This opens the way to even more complex configurations, such as those of half-integer (or spin type of fermionic) configurations, described in Mendonça et al. (2018). The road to topological studies of the supercontinuum is therefore open for exploration.

We have also briefly discussed the possible observation of superfluid light, which is related with the inhibition of diffraction above some critical intensity. This property is related with the inhibition of poloidal perturbations in the transverse direction. It is particularly relevant for twisted laser pulses because, in contrast with purely Gaussian pulses, they possess a transverse photon flow velocity proportional to the topological charge. Superfluidity is adequately described by a nonlinear Schrödinger equation, generally valid in Kerr media, from where appropriate fluid equations can be derived.

Transition between a normal fluid and superfluid light can be established using the celebrated Landau criterion. When applied to the present problem, this criterion depends on the laser pulse intensity and frequency profiles and is modified by the occurrence of SPM. Based on the Landau criterion, an intensity-distance map was established, where three different experimental regimes could be identified. They correspond to the observation of SPM and supercontinuum alone, to the observation of superfluidity alone, or to a yet unexplored new regime where SPM modifies the Landau criterion and nonlinear effects along the propagation direction can influence those in the perpendicular direction. This could bring new challenges and opportunities for the experimental work and for future optical applications.

References

Alfano, R. R. (2016). *The supercontinuum laser source* (3rd ed.). Springer.
Alfano, R. R., & Shapiro, S. L. (1970). *Physical Review Letters, 24, 584, 592*, 1217.
Bolda, E. L., Chiao, R. Y., & Zurek, W. H. (2001). *Physical Review Letters, 86*, 416.
Boyd, R. W. (1992). *Nonlinear optics*. Academic Press.
Carusoto, I., & Ciuti, C. (2013). *Reviews of Modern Physics, 85*, 299.

Chiao, R. Y., & Boyce, J. (1999). *Physical Review A, 60*, 4114.
Lerario, G., Fieramosca, A., Barachati, F., Ballarini, D., Daskalakis, K. S., Dominici, L., De Giorgi, M., Maier, S. A., Gigli, G., Kéna-Cohen, S., & Sanvitto, D. (2017). *Nature Physics, 13*, 837.
Mendonça, J. T. (2001). *Theory of photon acceleration*. Institute of Physics Publishing.
Mendonça, J. T. (2020). *Europhysics Letters, 129*, 64004.
Mendonça, J. T., & Vieira, J. (2014). *Physics of Plasmas, 21*, 033107.
Mendonça, J. T., Thidé, B., & Then, H. (2009). *Physical Review Letters, 102*, 185005.
Mendonça, J. T., Serbeto, A., & Vieira, J. (2018). *Scientific Reports, 8*, 7817.
Michel, C., Boughdad, O., Alber, M., Larré, P.-E., & Bellec, M. (2018). *Nature Communications, 9*, 2108.
Pariente, G., & Quéré, F. (2015). *Optics Letters, 40*, 2037.
Pethick, C. J., & Smith, H. (2008). *Bose-Einstein condensates in dilute gases* (2nd ed.). Cambridge University Press.
Rego, L., Dorney, K. M., Brooks, N. J., Nguyen, Q. L., Liao, C.-T., San Román, J., Couch, D. E., Liu, A., Pisanty, E., Lewenstein, M., Plaja, L., Kapteyn, H. C., Murnane, M. M., & Hernández-García, C. (2019). *Science, 364*, 1253.
Rodrigues, J. D., Mendonça, J. T., & Terças, H. (2020). *Physical Review A, 101*, 043810.
Secor, J., Alfano, R., & Ashrafi, S. (2017). *Complex light*. Institute of Physics Publishing.
Silva, N. A., Mendonça, J. T., & Guerreiro, A. (2017). *JOSA B, 34*, 2220.
Vieira, J., Mendonça, J. T., & Quéré, F. (2018). *Physical Review Letters, 121*, 054801.
Yao, A. M., & Padgett, M. J. (2011). *Advances in Optics and Photonics, 3*, 161.
Zhu, Z.-H., Chen, P., Li, H.-W., Zhao, B., Zhou, Z.-Y., Hu, W., Gao, W., Lu, Y.-Q., & Shi, B. S. (2018). *Applied Physics Letters, 112*, 161103.